Earth's Future

RESEARCH ARTICLE
10.1029/2025EF006789

How Will China's Surface Ozone Evolve Under Carbon Neutrality Target and Global Climate Warming?

Yue Tan[1,2], Tao Wang[1,2], Yiming Liu[3], Yingnan Zhang[1], Tianshu Chen[1], and Yurun Wang[1]

[1]State Key Laboratory of Climate Resilience for Coastal Cities, Department of Civil and Environmental Engineering, the Hong Kong Polytechnic University, Hong Kong, China, [2]The Hong Kong Polytechnic University Shenzhen Research Institute, Shenzhen, China, [3]School of Atmospheric Sciences, Sun Yat-sen University and Southern Marine Science and Engineering Guangdong Laboratory (Zhuhai), Zhuhai, China

Key Points:

- Emission cuts by pollution control and carbon neutrality policies would reduce MDA8 ozone by 31%–49% in China's key polluted regions by 2060
- In the short term, ozone may rebound or decline more slowly due to climate-driven accelerated ozone formation
- Ozone-temperature sensitivity would be reduced by half from 2020 to 2060 due to continuous anthropogenic emission control

Supporting Information:

Supporting Information may be found in the online version of this article.

Correspondence to:

T. Wang,
tao.wang@polyu.edu.hk

Citation:

Tan, Y., Wang, T., Liu, Y., Zhang, Y., Chen, T., & Wang, Y. (2026). How will China's surface ozone evolve under carbon neutrality target and global climate warming? *Earth's Future*, *14*, e2025EF006789. https://doi.org/10.1029/2025EF006789

Received 23 JUN 2025
Accepted 27 DEC 2025
Corrected 28 JAN 2026

This article was corrected on 28 JAN 2026. See the end of the full text for details.

Author Contributions:

Conceptualization: Yue Tan, Tao Wang
Data curation: Yue Tan
Formal analysis: Yue Tan, Tao Wang
Funding acquisition: Tao Wang
Investigation: Yue Tan
Methodology: Yue Tan, Yiming Liu
Resources: Tao Wang
Software: Yue Tan, Yiming Liu
Supervision: Tao Wang
Visualization: Yue Tan
Writing – original draft: Yue Tan, Tao Wang

Abstract Surface ozone (O_3) has complex relationships with its precursors and is also highly sensitive to meteorological variation and climate change. In China, ground-level ozone pollution remains a persistent air quality concern despite decreasing concentrations of other air pollutants in recent years. China's commitment to achieving carbon neutrality by 2060 is expected to result in unprecedented reductions in air pollutant emissions in the future. This study investigates the combined impacts of anthropogenic emission reductions and future climate change on the evolution of summertime surface O_3 under China's carbon neutrality target and the ambitious global 2°C warming scenario. Model simulations reveal an approximately 43% decline (range 31%–49%) in summertime daily maximum 8-hr average (MDA8) O_3 in China's six heavily polluted key regions from 2020 to 2060. However, risk of rebound is also projected in some near years due to weather-driven accelerated O_3 production rate, enhanced biogenic volatile organic compound (VOC) emissions and atmospheric stagnation, partially offsetting emission reduction benefits. The substantial aerosol reductions (by over 80%) would also enhance MDA8 O_3 (up to 10 ppb) from 2020 to 2060 primarily via heterogeneous reactions on aerosols. The high O_3-temperature sensitivity poses challenges to O_3 mitigation in the short term, with frequent heatwaves or droughts dampening the outcomes of ongoing anthropogenic emission control. In the long term, O_3-temperature sensitivity would be reduced by nearly half thanks to continuous anthropogenic emission control, thereby gradually increasing O_3 climatic resilience. Quicker and stronger emission control, especially for the anthropogenic VOCs, would significantly mitigate short-term rebound risks.

Plain Language Summary Ground-level ozone forms when gases from vehicles, factories, and plants react in warm and sunny weather. Despite progress on mitigating other air pollutants in China, ozone pollution remains challenging to control due to non-linear effect of its precursors, and impact of particulate matters and extreme weather. China's pledge to achieve carbon neutrality by 2060 will drastically cut human-made pollutant emissions. Our study projects that this would reduce peak summer ozone levels by about 43% in major cities by 2060. However, in the nearer future, ozone might temporarily *increase* in some areas due to increased occurrence of heatwaves and stagnant weather, which speeds up chemical reaction rates, increases plants' release of gases, and traps pollutants, offsetting early pollution control gains. This strong link between heat and ozone makes short-term control harder. Quicker, deeper cuts to gases from human activities, especially industry and vehicles, are needed to prevent this rebound.

1. Introduction

Surface ozone (O_3) is a major air pollutant that adversely affects human health and vegetation (e.g., T. Wang et al., 2017). In China, ground-level ozone pollution has drawn much concern due to persistently high O_3 concentrations in many urban and industrial regions, despite overall declines in other air pollutants (e.g., Y. Liu & Wang, 2020a; T. Wang et al., 2022; Y. Wang et al., 2020). The lingering ozone pollution problem arises from the non-linear response of O_3 to its precursors, its high sensitivity to meteorological variability, aerosol radiative effects, inter-regional transport and other related factors (Y. Liu & Wang, 2020a, 2020b; Lu et al., 2019; T. Wang et al., 2017, 2022; Xue et al., 2014). Recent studies have shown that substantial reductions in anthropogenic emissions of nitrogen oxides (NOx) and particulate matter (PM) following the implementation of China's Clean Air Action Plans in 2013 led to increases in surface ozone concentrations in many urban areas, primarily due to the NOx titration effect and the aerosol inhibition effect (K. Li et al., 2019; Y. Liu & Wang, 2020b; Y. Liu et al., 2023). Meteorological variability has also played varied but important roles in inter-annual changes in

Writing – review & editing: Yue Tan, Tao Wang, Yiming Liu, Yingnan Zhang, Tianshu Chen, Yurun Wang

surface ozone levels (Y. Liu & Wang, 2020a; Lu et al., 2019). Furthermore, a substantial body of research has documented increase in urban ozone concentrations during Covid-19 lockdowns, despite large reductions in emissions of almost all anthropogenic pollutants, as well as during recent extreme heatwave events (Chen et al., 2024; Tan et al., 2024; T. Wang et al., 2022). These findings underscore the complex responses of ozone to changes in emissions and meteorological conditions, posing significant challenges for policymakers in formulating and evaluating effective ozone control measures.

In 2020, China announced a series of climate mitigation policies, committing to the new goals of reaching carbon peak before 2030 and attaining carbon neutrality by 2060. This ambitious climate commitment, together with stringent pollution control polices, is projected to reduce CO_2 emissions by 15% and conventional pollutant emissions by 58%–67% by 2030 relative to 2015 levels, and to further reduce emissions of 92% for CO_2 and 67%–83% for conventional pollutants by 2060 compared to 2030 (Cheng et al., 2021). According to the latest reported data in China's National Bureau of Statistics (https://data.stats.gov.cn/english/), $PM_{2.5}$, NO_x, and SO_2 emissions had been reduced by 44%, 35%, and 87%, respectively, in 2023 compared to 2015, which will hopefully reach the anticipated reductions in 2030. Several modeling studies have demonstrated the potential benefits of these projected emission reductions in decreasing surface O_3 (by ∼50%) and $PM_{2.5}$ (by ∼70%) concentrations by 2060 under fixed meteorology conditions (Cheng et al., 2021, 2023; Hou et al., 2023; Qin et al., 2024; Shi et al., 2021). Another study, which assumed constant pollution emissions, examined the impact of extreme weathers under climate warming (RCP4.5) on O_3 and $PM_{2.5}$ and projected an increase in the respective population-weighed concentration by 3% and 4%, respectively, by the middle of the century (Hong et al., 2019). A recent study that considered both emission reductions and climate change attributed a decrease of 19 ppb in summertime surface O_3 during 2060–2070 primarily to emission reductions under a net-zero SSP1-19 pathway (Z. Liu et al., 2023). Previous studies have primarily focused on the ozone changes in the distant future. However, there is need to examine how surface ozone will evolve in the near future as well, considering changing anthropogenic emissions, climate variability, and O_3-climate sensitivity.

In this study, we examine changes in summertime O_3 and $PM_{2.5}$ concentrations, as well as their exceedance conditions, in China at 5-year intervals from 2020 to 2060, under the joint context of the optimistic global climate change and China's carbon neutrality policies. We assume that China would strictly adhere to its carbon neutrality pathway, and that globe efforts would be made to achieve the Paris Agreement's goal of limiting global warming to below 2°C (SSP1-2.6). We then disentangle the individual contributions of climate-induced meteorological variations and policy-driven emission reductions. The objective of this study is to determine whether, and to what extent, our anticipated emission control policies could fight against the adverse effects of climate warming on O_3 mitigation under optimistic scenarios. Additionally, given the increasing importance of the O_3 climate penalty under global warming, we also calculate O_3-temperature sensitivity to assess its future climatic resilience.

2. Materials and Methods

2.1. Model Configurations

The Community Multiscale Air Quality (CMAQ) Modeling System is designed to simulate and analyze air quality and its interactions with meteorology (Byun & Schere, 2006). This study used the offline CMAQ model (version 5.2.1) to project future summertime (June-July-August, JJA) O_3 and $PM_{2.5}$ concentrations in China from 2020 to 2060 at the intervals of 5 years (i.e., 2020, 2025, 2030, 2035,…, 2060), under both China's emission control scenarios (carbon neutrality) and global climate change scenarios (SSP1-2.6).

The future meteorological fields used in CMAQ model are generated using the Weather Research and Forecasting (WRF) model (version 4.2.1). The meteorological parameterization schemes applied in WRF model are listed in Table S1 in Supporting Information S1. The gas-phrase, aerosol, and liquid-phrase chemical schemes implemented in CMAQ model are SAPRC07tic, AERO6i, and AQKMTI, respectively. In addition, we updated the heterogeneous reactions based on previous work, including the addition of the uptake of HO_2, O_3, OH and H_2O_2 on the aerosol surface, as well as the updated heterogeneous reaction rates of NO_2 and NO_3 on the aerosol surface (Y. Liu & Wang, 2020a). The boundary conditions and initial conditions for chemical species in CMAQ are the default profiles, as the foreign impacts are relatively minor in the six target heavily polluted key regions (see Session 2.1.1) (J.-W. Xu et al., 2023). A spin-up period of 15 days prior to the study period (June 1st to August 31st) for each simulation is applied to minimize the impacts of initial conditions. The model performance is evaluated (see details in Text S1 in Supporting Information S1) and overall satisfactory to facilitate further

analysis of the relative contributions of climate-induced meteorological variations and policy-driven emission reductions. The uncertainties and limitations are discussed in detail in Text S2 in Supporting Information S1.

2.1.1. Model Domain and Region Classification

We conducted the CMAQ simulations over the land areas of China and its surrounding areas based on the Lambert conformal conic projection with a central origin at 110°E, 35°N and standard parallels at 15°N and 55°N (see Figure S1 in Supporting Information S1). The simulation domain extends from −3,078 km to 3,114 km in the *X* direction and from −2,286 km to 2,286 km in the *Y* direction. The entire domain has a horizontal resolution of 36 km × 36 km and includes 23 sigma layers vertically extending from the surface to the tropopause.

This study focuses on six heavily polluted key regions, which encompass the majority of urbanized and densely populated areas and megacities in China, to assess future air quality projections. These six key regions include Beijing-Tianjin-Hebei and Surroundings (BTHS), Yangtze River Delta (YRD), Pearl River Delta (PRD), Sichuan Basin (SCB), Fenwei Plain (FWP), and Triangle of Central China (TCC) (see detailed region definitions in Figure S1 and Table S3 in Supporting Information S1), similar to the region definitions in a previous study (Cheng et al., 2021). These regions are home to China's largest cities, such as Beijing, Shanghai and Guangzhou, as well as their most important manufacturing bases. The results for each key region in this study are averages over the model grids within the key region's boundary which includes the city cores and the much larger surrounding suburbs and rural areas under the city's jurisdiction, as defined by the shapefile derived from DataV.GeoAtlas platform (https://geo.datav.aliyun.com/areas_v3/bound/100000_full_city.json).

2.1.2. Meteorology Inputs

In this study, we assume that global efforts would be made to achieve the Paris Agreement's goal of limiting global warming to below 2°C. Additionally, we selected the Shared Socioeconomic Pathway1-2.6 (SSP1-2.6), developed by CMIP6 (the Coupled Model Intercomparison Project Phase 6) (O'Neill et al., 2016), as the climate scenario. To incorporate the long-term climate change into our simulations, future meteorological conditions were dynamically downscaled using WRF from the six-hourly data set produced by Max Planck Institute Earth System Model (etc., MPI-ESM1-2-HR) (Mauritsen et al., 2019), derived from the Coupled Model Intercomparison Project Phase 6 (CMIP6) models (Eyring et al., 2016) (https://esgf-metagrid.cloud.dkrz.de/search). We sampled nine evenly spaced years (2020, 2025,…, 2060) of meteorological fields to drive the dynamical downscaling, which could capture ∼84% (averaged by all the key regions, Figure S13 in Supporting Information S1) of the climate variability in 2 m temperature from 2020 to 2060 (see details in Text S2 in Supporting Information S1). The variables utilized include three-dimensional fields of air temperature, specific humidity, wind speed, geopotential height, as well as two-dimensional fields of surface pressure, 2-m temperature, 10-m wind speed, skin temperature, mean sea-level pressure, 2-m relative humidity, soil moisture, and soil temperature.

The MPI-ESM1-2-HR model was chosen due to its high resolution (six-hourly temporal resolution and 0.96° × 0.96° spatial resolution) and generally good performance on the atmospheric circulation and sea surface temperature of MPI-M Earth system model compared to other models in both CMIP5 and CMIP6 (Han et al., 2022; Huang et al., 2019; Richter & Tokinaga, 2020; Z. Xu et al., 2021). The MPI-ESM1-2 model has an equilibrium climate sensitivity (ECS) of 2.77°C to a CO_2 doubling over preindustrial conditions (Mauritsen et al., 2019), which is close to the median ECS (3.7°C) of CMIP6 model ensemble (very likely ranging 2–5°C) (Intergovernmental Panel on Climate Change (IPCC), 2023). This means MPI-ESM1-2-HR model projects a moderate warming response and its temperature-driven meteorological changes are broadly representative of the central tendency of CMIP6 models. The use of one specific model for dynamic downscaling, rather than an ensemble of multiple models, is justified by the fact that ensemble averaging may cancel out internal climate variability and thus reduce the temporal fluctuations of individual meteorological variable (Z. Xu et al., 2021).

2.1.3. Emission Inputs

The future anthropogenic emission inventory for mainland China was retrieved from the Dynamic Projection model for Emissions in China (DPEC) (Cheng et al., 2021, 2023; Tong et al., 2020) (http://meicmodel.org.cn/?page_id=1918&lang=en). We selected the on-time peak–net zero–clean air scenario in DPEC-v1.2 to evaluate future summertime air quality in China under a suite of policies targeting carbon peak, carbon neutrality and the best-health-effect (BAU) pollution control, under the future climate change scenario of SSP1-2.6. The

Table 1
Configurations of CMAQ Model Simulations

Case	Type	Meteorological field	Anthropogenic emission
M20E20	Base simulations	2020	2020
M25E25		2025	2025
M30E30		2030	2030
M35E35		2035	2035
M40E40		2040	2040
M45E45		2045	2045
M50E50		2050	2050
M55E55		2055	2055
M60E60		2060	2060
M20E25	Sensitivity experiments	2020	2025
M20E30		2020	2030
M20E35		2020	2035
M20E40		2020	2040
M20E45		2020	2045
M20E50		2020	2050
M20E55		2020	2055
M20E60		2020	2060

anthropogenic emissions used in our simulation include five sectors (i.e., transportation, resident, power, industry and agriculture), with shipping emissions not included. The anthropogenic emissions for regions outside mainland China and the other Asian countries were set as zero to isolate the effects of emission control within mainland China, as the impact of anthropogenic emissions outside mainland China on our results was shown to be marginal based on a sensitivity simulation (see details in Text S3 in Supporting Information S1). The biogenic emissions are calculated using the Model of Emissions of Gases and Aerosols from Nature (MEGAN) (Guenther et al., 2012) driven by the WRF meteorological output.

2.2. Experiment Settings

Nine base simulations were conducted for the summers (JJA) from 2020 to 2060 at 5-year intervals, using the corresponding meteorological fields and anthropogenic emissions of that year (i.e., M20E20, M25E25, M30E30, M35E35, M40E40, M45E45, M50E50, M55E55, M60E60) (see details in Table 1). To separate the effects of future climate changes and anthropogenic emission changes on air quality, eight additional sensitivity experiments are performed using the meteorological field of 2020 but with the anthropogenic emissions from different years (i.e., M20E25, M20E30, M20E35, M20E40, M20E45, M20E50, M20E55, M20E60) (see details in Table 1). The effects of anthropogenic emission changes are quantified by comparing the simulated concentrations for 2020 but with anthropogenic emissions of different years (e.g., M20E25-M20E20 for the year of 2025). The effects of climate changes are determined by comparing the base simulation concentrations of different years to those simulated for 2020 meteorological field but with the anthropogenic emissions of different years (e.g., M25E25-M20E25 for the year 2025).

To evaluate further the impact of future aerosol reduction on O_3 level, we have additionally conducted four sensitivity simulations (see details in Table 2). Using similar method in previous studies (K. Li et al., 2019; Y. Liu & Wang, 2020b), the impact of aerosols on O_3 via the change of photolysis rate is evaluated by comparing the effect of aerosols on O_3 in 2020 in terms of photolysis rates (M20E20-M20E20_nophot) to that in 2060 (M20E60-M20E60_nophot), fixing the impact of meteorological field. Similarly, the impact of aerosols on O_3 via all heterogeneous reactions on aerosol surface is evaluated by comparing the effect of aerosols on O_3 in 2020 in terms of heterogeneous reactions (M20E20-M20E20_het) to that in 2060 (M20E60-M20E60_nohet).

3. Results

3.1. Descending Trend but Potential Risk of Rebound

Figure 1 shows the summertime concentrations of daily maximum 8-hr average (MDA8) O_3 and 24-hr $PM_{2.5}$, along with their exceedance days from 2020 to 2060, across six key regions in China under future emission and climate change scenarios. Over this period, MDA8 O_3 is projected to decline by 42.67 ± 5.85% in these key regions, while $PM_{2.5}$ is projected to decrease more substantially–by over 80% (Figures 1a and 1b). The magnitude of decline exhibits considerable spatial heterogeneity, both among different key regions, and between these key regions and their surrounding less-urbanized areas. Notably, MDA8 O_3 in the BTHS region would decline by only 31.1%, significantly less than the reductions in the other five key regions (ranging from 41.5% to 49.4%), primarily due to the relatively broader VOC-limited areas inside BTHS (W. Wang et al., 2021) and its high initial O_3 level. Furthermore, MDA8 O_3 in these six key regions would remain prominent compared to surrounding less-urbanized areas throughout the study period (Figures 2a and 2b and Figure S4 in Supporting Information S1), highlighting the persistent challenges of O_3 control, especially in highly urbanized areas. The $PM_{2.5}$ hotspots in the BTHS, SCB, TCC and YRD regions would disappear by 2060 (Figures 2d and 2e), suggesting that summertime $PM_{2.5}$ control could hopefully be largely achieved by then. However, previous studies have shown that reductions in $PM_{2.5}$ could accelerate O_3 production through heterogeneous chemical and radiative effects (K. Li et al., 2019; Y. Liu & Wang, 2020b). In our study, the projected future reduction in PM from 2020 to 2060 would also enhance O_3

Table 2
Sensitivity Experiments to Evaluate Impact of Aerosol Reduction on O_3

Experiment	Description
M20E20_nophot	M20E20 but without aerosol impact through the change of photolysis rate
M20E20_nohet	M20E20 but without all heterogeneous reactions on aerosol surface
M20E60_nophot	M20E60 but without aerosol impact through the change of photolysis rate
M20E60_nohet	M20E60 but without all heterogeneous reactions on aerosol surface

formation especially in north China, primarily via heterogeneous reactions on aerosols (up to 10.7 ppb), as well as by altering photolysis rate albeit more mildly (Figure 3), posing additional challenge for O_3 control.

Our simulated long-term (till 2060) downward trend is consistent with previous studies that consider emission reductions under carbon neutrality with fixed meteorology (Cheng et al., 2021, 2023; Shi et al., 2021). However, despite the overall downward trend, our results also captured the risk of rebound in MDA8 O_3 (as well as $PM_{2.5}$ albeit more mildly) (Figures 1a and 1b), due to the inclusion of evolving meteorology fields (climate change) in our simulations. The most pronounced rebound would occur in 2040 (compared to 2035) in five regions (except YRD), with MDA8 O_3 increased by 1.12, 3.82, 3.41, 0.34, and 2.25 ppb in BTHS, PRD, SCB, FWP and TCC, respectively, while MDA8 O_3 would decrease slightly by 0.61 ppb in YRD. Besides, the decreasing rate of MDA8 O_3 would slow down in 2055 (compared to 2050) in YRD, FWP, and TCC, with a slight rebound (0.79 ppb) in YRD. These rebounds and slowed declines in MDA8 O_3 should be attributed to meteorological fluctuations, which is further discussed in Section 3.2.

In conjunction with the potential rebound, the exceedance conditions indicate that summertime surface O_3 will remain a hard nut to crack in the near future, especially in the BTHS and FWP regions. Although region-averaged MDA8 O_3 would meet China's National Ambient Air Quality Standards (NAAQS) for ozone (160 μg/m^3) throughout the study period, it would not fall below World Health Organization (WHO) standard (100 μg/m^3) until 2045 in the YRD, PRD and TCC regions, and until 2055 in the SCB region and until 2060 in the BTHS and FWP regions (Figure 1a). In contrast, $PM_{2.5}$ could meet the WHO 24-hr standard (etc., 15 μg/m^3) by 2045 in

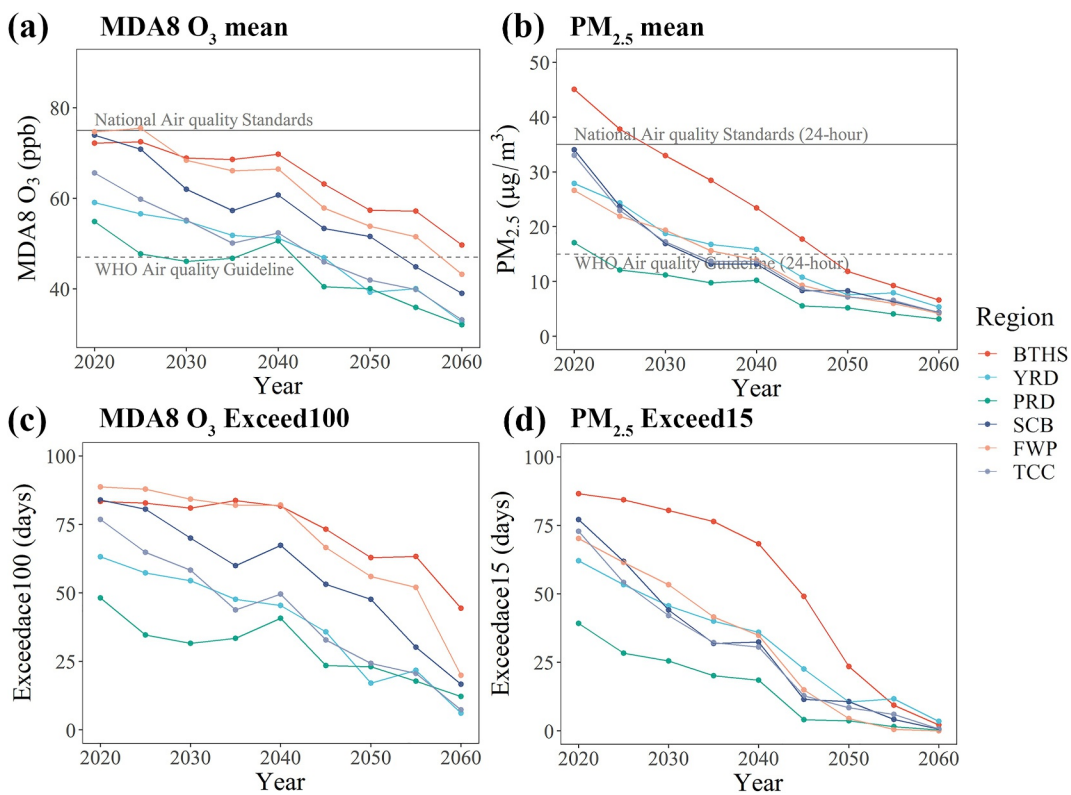

Figure 1. Temporal variation of summertime MDA8 O_3 (a), $PM_{2.5}$ (b), MDA8 O_3 Exceed100 (c) and $PM_{2.5}$ Exceed15 (d) during 2020–2060 at the interval of 5 years. The air quality limits for MDA8 O_3 in (a) is 160 μg/m^3 (~75 ppb) in China's National Air Quality Standards and 100 μg/m^3 (~47 ppb) in WHO Air Quality Guideline, which are converted to ppb under standard conditions (1,013 hPa, 273 K) (Lyu et al., 2023). The air quality limits for $PM_{2.5}$ in (b) is 35 μg/m^3 in China's National Air Quality Standards and 15 μg/m^3 in WHO Air Quality Guideline.

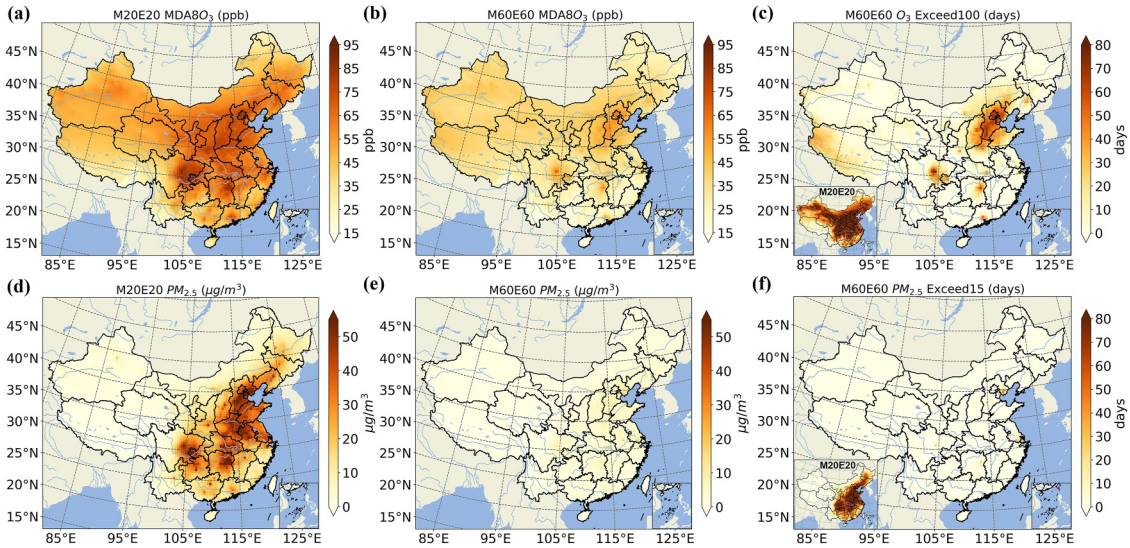

Figure 2. Spatial distribution of summertime MDA8 O_3 in 2020 (a) and 2060 (b), and MDA8 O_3 Exceed100 (c), and summertime $PM_{2.5}$ in 2020 (d) and 2060 (e), and $PM_{2.5}$ Exceed15 (f).

almost all six regions (except BTHS, expected to comply by 2050) (Figure 1b). To assess exceedance days, we calculated the number of days with MDA8 O_3 exceeding 100 μg/m^3 (MDA8 O_3 Exceed100) or 160 μg/m^3 (MDA8 O_3 Exceed160), and days with $PM_{2.5}$ exceeding 15 μg/m^3 ($PM_{2.5}$ Exceed15) or 35 μg/m^3 ($PM_{2.5}$ Exceed35) (Figures 1c and 1d and Figure S3 in Supporting Information S1). MDA8 O_3 Exceed100 would remain high before 2040 (61.1 days in 2040, 66.3% of the whole summertime), especially in BTHS (81.7 days, 88.8%) and in FWP (82.1 days, 89.3%), and then drop sharply (by ∼82%) to fewer than 20 days in 2060 in five regions, except BTHS (still up to 44.4 days, nearly half of the summer). The sharp drop of MDA8 O_3 exceedance days and its concentrations after 2040 is mainly due to the accumulating effects of synergistic emission control (see details in Section 3.2.1). In contrast, the outlook for $PM_{2.5}$ is more optimistic. By 2050, $PM_{2.5}$ Exceed15 would drop to ∼10 days in the other five regions, except for BTHS (still up to 23.5 days, 25.5%) (Figure 1d). By 2060, $PM_{2.5}$ Exceed15 would have decreased by around 98% compared to 2020 in all six regions, with almost no exceedance days for $PM_{2.5}$ (Figures 1d and 2f).

3.2. Interacting Contributions: Emission Reduction and Climate Change

3.2.1. Accumulating Contributions of Emission Reduction

The anthropogenic emissions of O_3 precursors, including NOx and non-methane volatile organic compounds (NMVOCs), are projected to decrease in the future, as indicated by previous studies (Cheng et al., 2021, 2023;

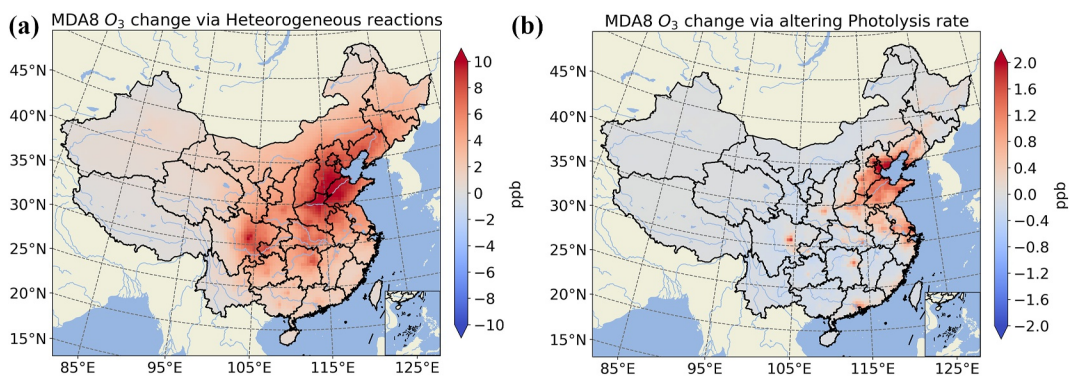

Figure 3. The simulated MDA8 O_3 change in response to summertime aerosol reductions from 2020 to 2060 via (a) heterogeneous reactions and (b) altering photolysis rate.

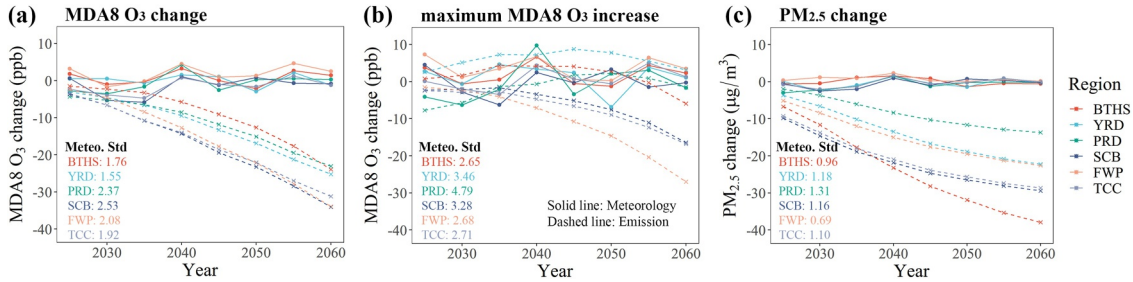

Figure 4. The contribution of meteorological change and emission reductions to MDA8 O_3 change (a), maximum value of MDA8 O_3 increase relative to 2020 (b) and $PM_{2.5}$ change (c) during 2025–2060 in comparison to 2020. The solid lines represent the changes of MDA8 O_3 or $PM_{2.5}$ due to the meteorological change, and the dashed lines represent those due to the anthropogenic emission change (reduction) in the years of 2025, 2030, 2035, …, 2060, relative to the year 2020. The "Metro. Std" at the left-bottom of each panel represents the standard deviation of the contribution of meteorological change.

Tong et al., 2020). Here, we calculated total anthropogenic emissions (projected by DPEC) during summertime from 2020 to 2060 within the six key regions (Figure S10 in Supporting Information S1). Emissions of both NOx and NMVOC (primarily distributed in BTHS, YRD and PRD) are projected to decrease sharply in the early stage (2020–2040), followed by a slower decline after 2040 (Figure S10a in Supporting Information S1). Despite the diminishing descent rate for both NOx and NMVOC after 2040, the reduction rate of NOx emissions (−0.39 g/m^2/decade) would turn quicker than that of NMVOC emissions (−0.35 g/m^2/decade), resulting in a sharp rise in the ratio of NMVOC emissions to NOx emissions (from 1.78 to 4.18 during 2040–2060, on average) after a slight increase during 2020–2040 (Figure S10b in Supporting Information S1). This indicates that NOx and NMVOC emission reductions would proceed in parallel in the early stage (2020–2040), with a greater emphasis on NOx control after 2040. This emission reduction pathway is effective, as both VOC and NOx should be controlled simultaneously under a VOC-limited O_3 formation regime in the early stage, with the focus shifting to NOx control under a NOx-limited regime in later years (T. Wang et al., 2022).

To isolate the contributions of anthropogenic emission reduction and climate change to changes in MDA8 O_3 and 24-hr $PM_{2.5}$ during 2025–2060 (at 5-year intervals) relative to 2020, a series of sensitivity experiments were conducted in addition to the baseline simulations (see details in Section 2.2). Figure 4 shows the separate contributions of anthropogenic emission reduction and climate change (including associate biogenic emission changes) to changes in summertime MDA8 O_3 and 24-hr $PM_{2.5}$ during 2025–2060, compared to 2020, with part of their spatial distributions in Figure 5. On average, for all the key regions, anthropogenic emission reduction would result in a gradual decline in MDA8 O_3 levels in the early period (2025–2040), followed by a more rapid decrease in the later period (2045–2060), under the on-time peak–net zero–clean air scenario. In contrast, $PM_{2.5}$ would decline rapidly initially, followed by a slower reduction in subsequent period (Figures 4a and 4c). This suggests that significant potential for O_3 mitigation would remain beyond 2060, and continued targeted emission controls (especially of NOx) would remain necessary for further O_3 mitigation. The different trajectories in O_3 and $PM_{2.5}$ are mainly due to their different formation mechanisms and the aforementioned different reduction pathways of NOx, NMVOC and $PM_{2.5}$ emissions. Considering the non-linear relationship of O_3 and its precursors, the rapid decrease in O_3 in the later period is because of continuous NO_x control when O_3 formation regimes gradually turn into NO_x-limited. While $PM_{2.5}$ would decrease more quickly in the early period because $PM_{2.5}$ emissions would reduce sharply before 2040, followed by slower decreasing trend afterward (Figure S10 in Supporting Information S1).

Additionally, anthropogenic emission reduction would conversely increase MDA8 O_3 in some VOC-limited regions, particularly in the early stage (2030–2045) in BTHS and YRD (Figure S5 in Supporting Information S1), due to the well-known NO titration effect (T. Wang et al., 2017, 2022). As shown in Figure 4b, we identified the hotspot grids with the maximum value of MDA8 O_3 increase in each simulation during 2025–2060 relative to 2020 in each key region to examine how the contributions of anthropogenic emission reduction and meteorological change would evolve in these areas. The contribution of emission reduction is projected to increase gradually, reach peaks (e.g., 4.32 ppb in BTHS in 2035, and 8.77 ppb in YRD in 2045), and then decrease in these hotspot grids. The increase in MDA8 O_3 in these VOC-limited regions could offset the overall reduction effect across the entire region due to anthropogenic emission reduction, partially explaining the slow decline in MDA8 O_3 in the early stage.

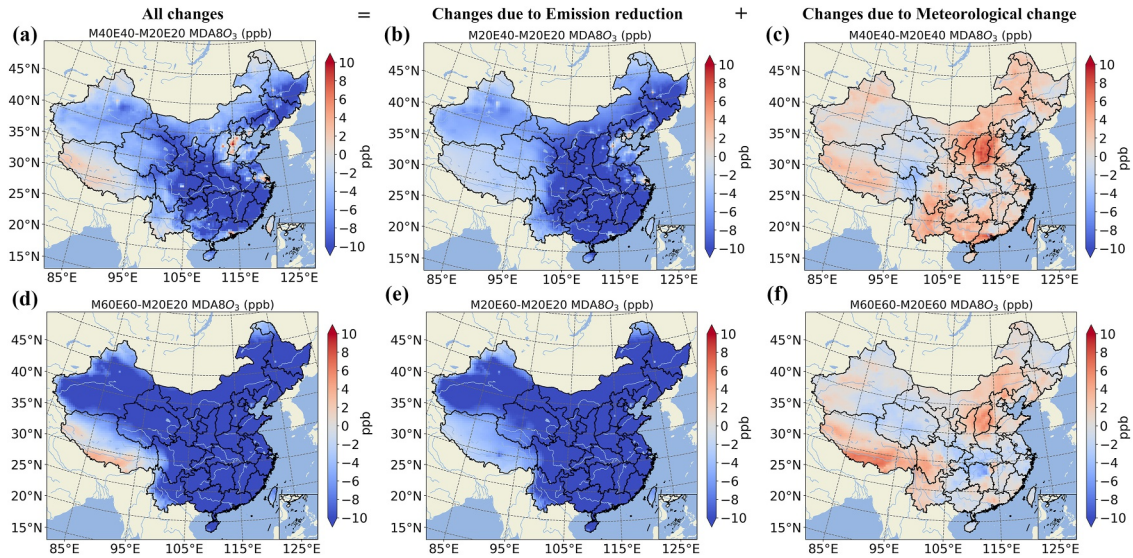

Figure 5. Spatial distribution of summertime MDA8 O_3 changes and the contributions due to emission reduction and meteorological change of 2040 (a, b, c) and 2060 (d, e, f) in comparison to 2020.

3.2.2. Fluctuating Contributions of Climate Change

The contribution of climate change under the SSP1-2.6 scenario could be more characterized as *fluctuations* compared with the clear trend in the contribution of anthropogenic emission control (Figures 4a and 4c and Figure S15 in Supporting Information S1). However, such fluctuations would certainly influence the effectiveness of the anthropogenic emission control policies on the summertime MDA8 O_3, especially in the short term. For instance, the contributions of meteorological change to MDA8 O_3 changes would offset the benefits of emission reductions, across almost the whole China, in 2040 compared to 2035 (Figure S6 in Supporting Information S1). As shown in Figure 4a, the contribution of meteorological change is projected to shift from negative values in 2035 (ranging from −5.82 to −0.16 ppb, averaged by −2.22 ppb) to quite positive values in 2040 (ranging from 0.80 to 4.49 ppb, averaged by 2.58 ppb) in all six key regions. In contrast, the negative contribution from emission control would deepen by just −3.07 ppb on average from 2035 to 2040, offset by the aforementioned enhanced positive contribution from meteorological change (by +4.79 ppb), similar to the situation (slowed decreasing rate) in 2055 compared to 2050.

This enhanced positive contribution of meteorological change to summertime MDA8 O_3 concentrations in 2040 relative to 2035 could be attributed mainly to two mechanisms, accelerated O_3 production rate and enhanced atmospheric stagnation. The accelerated O_3 production rate would dominate the central China, driven by higher temperature, lower relative humidity, stronger solar radiation reaching the ground surface and higher BVOC emissions in 2040 compared to 2035 (Figures S7a–S7c, and S7g in Supporting Information S1). Specifically, 2m temperature would increase significantly by 0.99, 0.60, 1.20, and 0.51°C in BTHS, SCB, FWP, and TCC, respectively (Figure S8a in Supporting Information S1). Consequently, total emissions of isoprene (ISOP), the most abundant BVOC, would increase by 0.39, 0.45, and 0.27 g/m^2 (or 13.7%, 17.8%, and 8.3%), in SCB, FWP, and TCC (regions with relatively high vegetation coverage), respectively (Figure S9 in Supporting Information S1). ISOP emissions would not increase substantially in BTHS (merely 0.14 g/m^2) due to its low vegetation coverage, despite the notable temperature rise. Relative humidity would decrease by 7.47%, 3.33% and 2.52% in SCB, FWP and TCC, respectively. Solar radiation reaching the ground surface would increase by 21.32, 12.90, and 16.77 W/m^2 in SCB, FWP and TCC, respectively.

Enhanced atmospheric stagnation would dominate the southeast China, with lower wind speed and lower planetary boundary layer (PBL) (Figures S7d and S7e in Supporting Information S1). Wind speed is projected to decrease apparently by 0.25, 0.52, and 0.27 m/s in YRD, PRD and TCC, respectively. The PBL would decrease by 13.82, 16.04 and 31.30 m in BTHS, YRD, and PRD, respectively (Figure S8 in Supporting Information S1). In

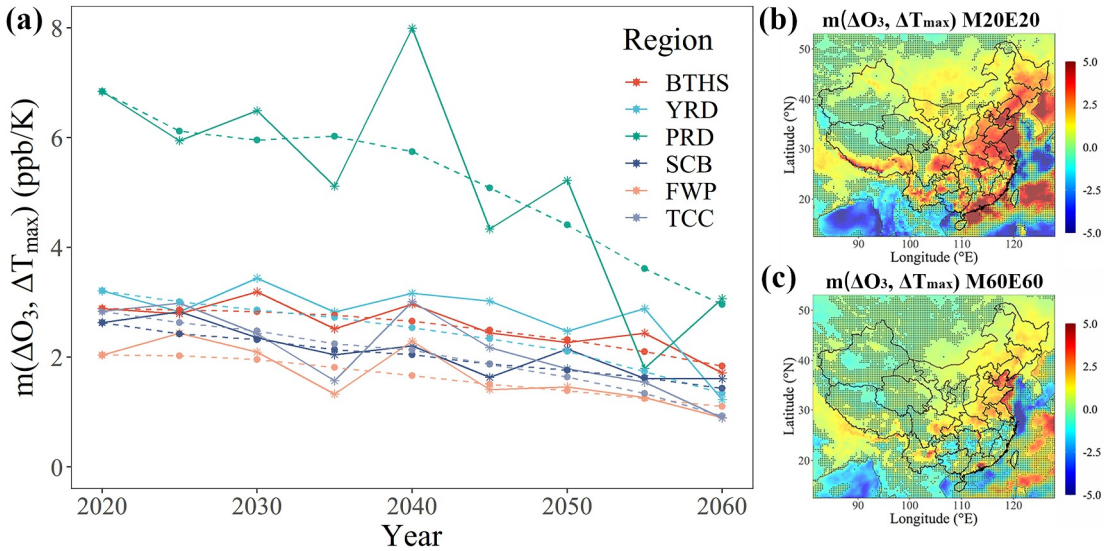

Figure 6. Evolution of summertime O_3 climate penalty ($m_{\Delta O3,\Delta Tmax}$) during 2020–2060 (a). The dashed lines represent the m(ΔO_3, ΔT_{max}) in the sensitivity experiments (M20E20, M20E25, M20E30, M20E35, M20E40, M20E45, M20E50, M20E55, M20E60), and the solid lines represent the $m(\Delta O_3, \Delta T_{max})$ in the base experiments (M20E20, M25E25, M30E30, M35E35, M40E40, M45E45, M50E50, M55E55, M60E60). Spatial distribution of summertime $m_{\Delta O3,\Delta Tmax}$ in 2020 (b) and 2060 (c). The dots denote grids where $m_{\Delta O3,\Delta Tmax}$ is statistically *insignificant* at the 95% confidence level, as determined by *t*-test.

addition, total summertime precipitation would decrease in five key regions (except BTHS) by 1.79, 6.40, 26.41, 3.83, and 9.54 cm in YRD, PRD, SCB, FWP, and TCC, respectively, leading to reduced wet deposition of O_3.

Despite the apparent rebound in MDA8 O_3, $PM_{2.5}$ would instead just hold the line in 2040 compared to 2035 (Figure 1b), with only a slight increase in the contribution from meteorological changes (+2.15 μg/m^3 on average), partially offsetting the intensified negative contribution of emission control (−3.33 μg/m^3) on $PM_{2.5}$. A possible reason is that meteorological changes enhance $PM_{2.5}$ just by atmospheric stagnation (lower wind speed and lower PBL height, Figure S7 in Supporting Information S1). The production rate of $PM_{2.5}$ may not increase substantially, as lower relative humidity inhibits the formation and hygroscopic growth of particles, although higher temperature may promote the formation of certain species of secondary particular matters (Colle et al., 2008; Thomsen et al., 2024). A previous study (Cheng et al., 2021) also reported relatively small impacts of meteorological fluctuations on $PM_{2.5}$ exposure in 2030 and 2060 under the Ambitious-pollution-2°C-goals scenario, indicating the relatively low climate sensitivity of $PM_{2.5}$. Therefore, compared with $PM_{2.5}$, the challenge in O_3 pollution control is primarily due to its high sensitivity to temperature, that is, O_3 climate penalty (Lu et al., 2019), which increases the risk of rebound in MDA8 O_3 in the short term.

Expanding from the "micro" scope (2035–2040) to the wider scope (2020–2060), contributions of climate change to MDA8 O_3 enhancement are projected to increase (Figures 4a and 5f, and Figure S15 in Supporting Information S1), driven by the anticipated rise in temperature (by 0.83°C on average across the six key regions from 2020 to 2060) under SSP1-2.6 (Figure S8a in Supporting Information S1), and the subsequent rising BVOC emissions (e.g., ∼10% increase in ISOP emissions) (Figures S9 and S11 in Supporting Information S1). But fortunately, the increasing and fluctuating contribution of meteorological changes would certainly be fully offset by the accumulating effects of emission reductions in the far future (after 2040) (Figure 4a).

3.3. From Short-Term Challenge to Long-Term Opportunity: The Descending O_3 Climate Penalty

Given the high sensitivity of O_3 to temperature, in order to examine how the future O_3 climate sensitivity would evolve, we calculated the summertime O_3-temperature sensitivity as the slope ($m_{\Delta O3,\Delta Tmax}$) of the best-fit line of daily MDA8 O_3 anomaly (ΔO_3) versus daily maximum temperature anomaly (ΔT_{max}) (see details in Text S4 in Supporting Information S1). As shown in Figure 6 and Figure S12 in Supporting Information S1, $m_{\Delta O3,\Delta Tmax}$ is projected to decrease by nearly half from 2020 to 2060 (from 2.0 to 6.8 ppb/°C to 0.9–3.0 ppb/°C), with a mean decreasing rate of −0.46 ppb/°C/decade, based on simulations using emissions of each respective year but with meteorological field fixed at 2020 (dashed lines, R: 0.37–0.76, *p*-value <0.05). This indicates that the

anthropogenic emission reductions (especially NOx reductions) would significantly decrease the O_3-temperature sensitivity in China in the future, which is consistent with the historical downward trends in the United States during the period of rapid emission control (Fu et al., 2015; S. Li et al., 2024; Rasmussen et al., 2013; Yin et al., 2025). Therefore, the projected future downward trend of $m_{\Delta O3,\Delta Tmax}$ due to anthropogenic emission reductions would gradually enhance O_3 climatic resilience and facilitate its mitigation in China in the farther future. One apparent evidence in our results is that despite higher temperature increases in 2055 (by 0.58°C in 2040 and 0.83°C in 2055, compared to their preceding 5th years), MDA8 O_3 would rise only slightly in one key region (by 0.79 ppb in YRD), or its descending rate would just slow down in other key regions in 2055, while it would rebound in almost all key regions (by up to 1.72 ppb on average) in 2040.

It is also notable that greater interannual fluctuations, especially in PRD, are projected when meteorological variations are included in simulations using both emissions and meteorological fields of each respective year (solid lines, R: 0.35–0.74, p value <0.05), although the overall trend in $m_{\Delta O3,\Delta Tmax}$ is consistent with the above trend. We infer that such fluctuations in $m_{\Delta O3,\Delta Tmax}$ may be introduced by interannual variations in regional ozone advection and the dispersion conditions. Another possible reason is changes in the O_3 formation regime resulting from the weather-induced BVOC emission variability. Similar large interannual variability was also observed in the southeast United States (Fu et al., 2015), where it was attributed primarily to variations in O_3 advection coupled with large-scale warming. Besides, $m_{\Delta O3,\ \Delta Tmax}$ is considerably higher in PRD compared to other key regions because it has both high local anthropogenic emissions (NOx and VOCs, Figure S10a in Supporting Information S1) and high local and surrounding vegetation coverage with high BVOC emissions (Figures S9a and S11 in Supporting Information S1) (Zanis et al., 2022).

4. Conclusion

Our study demonstrates a drastic decline in summertime MDA8 O_3 across heavily polluted key regions in China from 2020 to 2060 under CMIP6 (SSP1-2.6) climate projections and future emissions estimated from on-time peak–net zero–clean scenario. In the long term (after 2045), the benefits of continuous emission reductions are strong and promising, effectively offsetting the MDA8 O_3 enhancement due to global warming under SSP1-2.6. However, in the short term (e.g., before 2040), MDA8 O_3 may rebound, or its descending rate may slow down in certain years, due to weather-induced accelerated O_3 production, increased BVOC emissions and enhanced atmospheric stagnation. Besides, though MDA8 O_3 is projected to meet the NAAQS soon, achieving the more stringent WHO standards would remain challenging, with exceedance conditions lingering until 2045 and even later (till 2060) in the most developed key region (e.g., BTHS). Quicker and stronger emission control, especially for the anthropogenic VOC, would help prevent the short-term rebound risk and reduce the exceedance days. Our results also show that the emission control would gradually weaken the summertime O_3-temperature sensitivity by half by 2060, suggesting that mitigation strategies could be more resilient to increasingly frequent extreme weather.

While substantial improvements in surface ozone are projected under the optimistic SSP1-2.6 pathway, future climate remains quite uncertain and subject to the progress of global cooperation in implementing carbon policies, which may not go as planned. Global climate extremes may be more severe than anticipated, as evidenced by the recent increase in extreme weather events (e.g., heatwaves, drought and atmospheric stagnation) (Ebi et al., 2021; Newman & Noy, 2023), which would complicate future ozone improvement trends. Therefore, it is critical that the strict pollutant and carbon reduction policies be fully implemented to counteract climate warming induced ozone increase.

Conflict of Interest

The authors declare no conflicts of interest relevant to this study.

Data Availability Statement

The future emission inventories of major air pollutants (DPEC data) were available at http://meicmodel.org.cn/?page_id=1918&lang=en (Version 1.2, "on-time_peak-net_zero-clean_air," Cheng et al., 2023). The future meteorological fields by Max Planck Institute Earth System Model are available at https://esgf-metagrid.cloud.dkrz.de/search, searching by "Source ID = MPI-ESM1-2-HR" (Jungclaus et al., 2019). The hourly air pollutants

observation data of air pollutants are available at https://quotsoft.net/air/, by clicking on the indicator "Download China Air Quality Data from Baidu network disk." The hourly meteorological observations are available at https://www.ncei.noaa.gov/pub/data/noaa/isd-lite/ (Smith et al., 2011). The WRF model source code can be downloaded at https://www2.mmm.ucar.edu/wrf/users/download/get_sources.html. The CMAQ model source code can be downloaded at https://github.com/USEPA/CMAQ. Due to model output size limitation, specific model output requests can be made to the corresponding author.

Acknowledgments
This research was supported by the National Natural Science Foundation of China (42293322).

References

Byun, D., & Schere, K. L. (2006). Review of the governing equations, computational algorithms, and other components of the models-3 Community Multiscale Air Quality (CMAQ) Modeling System. *Applied Mechanics Reviews*, *59*(2), 51–77. https://doi.org/10.1115/1.2128636

Chen, T., Wang, T., Xue, L., & Brasseur, G. (2024). Heatwave exacerbates air pollution in China through intertwined climate-energy-environment interactions. *Science Bulletin*, *69*(17), 2765–2775. https://doi.org/10.1016/j.scib.2024.05.018

Cheng, J., Tong, D., Liu, Y., Geng, G., Davis, S. J., He, K., & Zhang, Q. (2023). A synergistic approach to air pollution control and carbon neutrality in China can avoid millions of premature deaths annually by 2060. *One Earth*, *6*(8), 978–989. https://doi.org/10.1016/j.oneear.2023.07.007

Cheng, J., Tong, D., Zhang, Q., Liu, Y., Lei, Y., Yan, G., et al. (2021). Pathways of China's $PM_{2.5}$ air quality 2015–2060 in the context of carbon neutrality. *National Science Review*, *8*(12), nwab078. https://doi.org/10.1093/nsr/nwab078

Colle, S., Vanderschuren, J., & Thomas, D. (2008). Effect of temperature on SO_2 absorption into sulphuric acid solutions containing hydrogen peroxide. *Chemical Engineering and Processing: Process Intensification*, *47*(9), 1603–1608. https://doi.org/10.1016/j.cep.2007.08.014

Ebi, K. L., Vanos, J., Baldwin, J. W., Bell, J. E., Hondula, D. M., Errett, N. A., et al. (2021). Extreme weather and climate change: Population health and health system implications. *Annual Review of Public Health*, *42*(1), 293–315. https://doi.org/10.1146/annurev-publhealth-012420-105026

Eyring, V., Bony, S., Meehl, G. A., Senior, C. A., Stevens, B., Stouffer, R. J., & Taylor, K. E. (2016). Overview of the Coupled Model Intercomparison Project Phase 6 (CMIP6) experimental design and organization. *Geoscientific Model Development*, *9*(5), 1937–1958. https://doi.org/10.5194/gmd-9-1937-2016

Fu, T.-M., Zheng, Y., Paulot, F., Mao, J., & Yantosca, R. M. (2015). Positive but variable sensitivity of August surface ozone to large-scale warming in the southeast United States. *Nature Climate Change*, *5*(5), 454–458. https://doi.org/10.1038/nclimate2567

Guenther, A. B., Jiang, X., Heald, C. L., Sakulyanontvittaya, T., Duhl, T., Emmons, L. K., & Wang, X. (2012). The model of emissions of gases and aerosols from nature version 2.1 (MEGAN2.1): An extended and updated framework for modeling biogenic emissions. *Geoscientific Model Development*, *5*(6), 1471–1492. https://doi.org/10.5194/gmd-5-1471-2012

Han, Y., Zhang, M.-Z., Xu, Z., & Guo, W. (2022). Assessing the performance of 33 CMIP6 models in simulating the large-scale environmental fields of tropical cyclones. *Climate Dynamics*, *58*(5–6), 1683–1698. https://doi.org/10.1007/s00382-021-05986-4

Hong, C., Zhang, Q., Zhang, Y., Davis, S. J., Tong, D., Zheng, Y., et al. (2019). Impacts of climate change on future air quality and human health in China. *Proceedings of the National Academy of Sciences*, *116*(35), 17193–17200. https://doi.org/10.1073/pnas.1812881116

Hou, X., Wild, O., Zhu, B., & Lee, J. (2023). Future tropospheric ozone budget and distribution over East Asia under a net-zero scenario. *Atmospheric Chemistry and Physics*, *23*(24), 15395–15411. https://doi.org/10.5194/acp-23-15395-2023

Huang, F., Xu, Z., & Guo, W. (2019). Evaluating vector winds in the Asian-Australian monsoon region simulated by 37 CMIP5 models. *Climate Dynamics*, *53*(1–2), 491–507. https://doi.org/10.1007/s00382-018-4599-z

Intergovernmental Panel on Climate Change (IPCC). (2023). The Earth's energy budget, climate feedbacks and climate sensitivity. In *Climate Change 2021—The Physical Science Basis: Working Group I Contribution to the Sixth Assessment Report of the Intergovernmental Panel on Climate Change* (pp. 923–1054). Cambridge University Press. https://doi.org/10.1017/9781009157896.009

Jungclaus, J., Bittner, M., Wieners, K.-H., Wachsmann, F., Schupfner, M., Legutke, S., et al. (2019). MPI-M MPIESM1.2-HR model output prepared for CMIP6 CMIP [Dataset]. *Earth System Grid Federation*. https://doi.org/10.22033/ESGF/CMIP6.741

Li, K., Jacob, D. J., Liao, H., Shen, L., Zhang, Q., & Bates, K. H. (2019). Anthropogenic drivers of 2013–2017 trends in summer surface ozone in China. *Proceedings of the National Academy of Sciences of the United States of America*, *116*(2), 422–427. https://doi.org/10.1073/pnas.1812168116

Li, S., Lu, X., & Wang, H. (2024). Anthropogenic emission controls reduce summertime ozone-temperature sensitivity in the United States. *EGUsphere*, 1–27. https://doi.org/10.5194/egusphere-2024-1889

Liu, Y., Geng, G., Cheng, J., Liu, Y., Xiao, Q., Liu, L., et al. (2023). Drivers of increasing ozone during the two phases of clean air actions in China 2013–2020. *Environmental Science & Technology*, *57*(24), 8954–8964. https://doi.org/10.1021/acs.est.3c00054

Liu, Y., & Wang, T. (2020a). Worsening urban ozone pollution in China from 2013 to 2017—Part 1: The complex and varying roles of meteorology. *Atmospheric Chemistry and Physics*, *20*(11), 6305–6321. https://doi.org/10.5194/acp-20-6305-2020

Liu, Y., & Wang, T. (2020b). Worsening urban ozone pollution in China from 2013 to 2017—Part 2: The effects of emission changes and implications for multi-pollutant control. *Atmospheric Chemistry and Physics*, *20*(11), 6323–6337. https://doi.org/10.5194/acp-20-6323-2020

Liu, Z., Wild, O., Doherty, R. M., O'Connor, F. M., & Turnock, S. T. (2023). Benefits of net-zero policies for future ozone pollution in China. *Atmospheric Chemistry and Physics*, *23*(21), 13755–13768. https://doi.org/10.5194/acp-23-13755-2023

Lu, X., Zhang, L., & Shen, L. (2019). Meteorology and climate influences on tropospheric ozone: A review of natural sources, chemistry, and transport patterns. *Current Pollution Reports*, *5*(4), 238–260. https://doi.org/10.1007/s40726-019-00118-3

Lyu, X., Li, K., Guo, H., Morawska, L., Zhou, B., Zeren, Y., et al. (2023). A synergistic ozone-climate control to address emerging ozone pollution challenges. *One Earth*, *6*(8), 964–977. https://doi.org/10.1016/j.oneear.2023.07.004

Mauritsen, T., Bader, J., Becker, T., Behrens, J., Bittner, M., Brokopf, R., et al. (2019). Developments in the MPI-M Earth system model version 1.2 (MPI-ESM1.2) and its response to increasing CO_2. *Journal of Advances in Modeling Earth Systems*, *11*(4), 998–1038. https://doi.org/10.1029/2018MS001400

Newman, R., & Noy, I. (2023). The global costs of extreme weather that are attributable to climate change. *Nature Communications*, *14*(1), 6103. https://doi.org/10.1038/s41467-023-41888-1

O'Neill, B. C., Tebaldi, C., van Vuuren, D. P., Eyring, V., Friedlingstein, P., Hurtt, G., et al. (2016). The Scenario Model Intercomparison Project (ScenarioMIP) for CMIP6. *Geoscientific Model Development*, *9*(9), 3461–3482. https://doi.org/10.1029/gmd-9-3461-2016

Qin, Y., Zhou, M., Hao, Y., Huang, X., Tong, D., Huang, L., et al. (2024). Amplified positive effects on air quality, health, and renewable energy under China's carbon neutral target. *Nature Geoscience*, *17*(5), 1–8. https://doi.org/10.1038/s41561-024-01425-1

Rasmussen, D. J., Hu, J., Mahmud, A., & Kleeman, M. J. (2013). The ozone–climate penalty: Past, present, and future. *Environmental Science & Technology*, *47*(24), 14258–14266. https://doi.org/10.1021/es403446m

Richter, I., & Tokinaga, H. (2020). An overview of the performance of CMIP6 models in the Tropical Atlantic: Mean state, variability, and remote impacts. *Climate Dynamics*, *55*(9–10), 2579–2601. https://doi.org/10.1007/s00382-020-05409-w

Shi, X., Zheng, Y., Lei, Y., Xue, W., Yan, G., Liu, X., et al. (2021). Air quality benefits of achieving carbon neutrality in China. *Science of the Total Environment*, *795*, 148784. https://doi.org/10.1016/j.scitotenv.2021.148784

Smith, A., Lott, N., & Vose, R. (2011). The integrated surface database: Recent developments and partnerships. *Bulletin of the American Meteorological Society*, *92*(6), 704–708. https://doi.org/10.1175/2011BAMS3015.1

Tan, Y., Zhang, Y., Wang, T., Chen, T., Mu, J., & Xue, L. (2024). Dissecting drivers of ozone pollution during the 2022 multicity lockdowns in China sheds light on future control direction. *Environmental Science & Technology*, *58*(16), 6988–6997. https://doi.org/10.1021/acs.est.4c01197

Thomsen, D., Iversen, E. M., Skønager, J. T., Luo, Y., Li, L., Roldin, P., et al. (2024). The effect of temperature and relative humidity on secondary organic aerosol formation from ozonolysis of Δ3-carene. *Environmental Sciences: Atmospheres*, *4*(1), 88–103. https://doi.org/10.1039/D3EA00128H

Tong, D., Cheng, J., Liu, Y., Yu, S., Yan, L., Hong, C., et al. (2020). Dynamic projection of anthropogenic emissions in China: Methodology and 2015–2050 emission pathways under a range of socio-economic, climate policy, and pollution control scenarios. *Atmospheric Chemistry and Physics*, *20*(9), 5729–5757. https://doi.org/10.5194/acp-20-5729-2020

Wang, T., Xue, L., Brimblecombe, P., Lam, Y. F., Li, L., & Zhang, L. (2017). Ozone pollution in China: A review of concentrations, meteorological influences, chemical precursors, and effects. *Science of the Total Environment*, *575*, 1582–1596. https://doi.org/10.1016/j.scitotenv.2016.10.081

Wang, T., Xue, L., Feng, Z., Dai, J., Zhang, Y., & Tan, Y. (2022). Ground-level ozone pollution in China: A synthesis of recent findings on influencing factors and impacts. *Environmental Research Letters*, *17*(6), 063003. https://doi.org/10.1088/1748-9326/ac69fe

Wang, W., Van Der A, R., Ding, J., Van Weele, M., & Cheng, T. (2021). Spatial and temporal changes of the ozone sensitivity in China based on satellite and ground-based observations. *Atmospheric Chemistry and Physics*, *21*(9), 7253–7269. https://doi.org/10.5194/acp-21-7253-2021

Wang, Y., Gao, W., Wang, S., Song, T., Gong, Z., Ji, D., et al. (2020). Contrasting trends of $PM_{2.5}$ and surface-ozone concentrations in China from 2013 to 2017. *National Science Review*, *7*(8), 1331–1339. https://doi.org/10.1093/nsr/nwaa032

Xu, J.-W., Lin, J., Tong, D., & Chen, L. (2023). The underappreciated role of transboundary pollution in future air quality and health improvements in China. *Atmospheric Chemistry and Physics*, *23*(17), 10075–10089. https://doi.org/10.5194/acp-23-10075-2023

Xu, Z., Han, Y., Tam, C.-Y., Yang, Z.-L., & Fu, C. (2021). Bias-corrected CMIP6 global dataset for dynamical downscaling of the historical and future climate (1979–2100). *Scientific Data*, *8*(1), 293. https://doi.org/10.1038/s41597-021-01079-3

Xue, L. K., Wang, T., Gao, J., Ding, A. J., Zhou, X. H., Blake, D. R., et al. (2014). Ground-level ozone in four Chinese cities: Precursors, regional transport and heterogeneous processes. *Atmospheric Chemistry and Physics*, *14*(23), 13175–13188. https://doi.org/10.5194/acp-14-13175-2014

Yin, L., Bai, B., Zhang, B., Zhu, Q., Di, Q., Requia, W. J., et al. (2025). Regional-specific trends of $PM_{2.5}$ and O_3 temperature sensitivity in the United States. *npj Climate and Atmospheric Science*, *8*(1), 1–15. https://doi.org/10.1038/s41612-024-00862-4

Zanis, P., Akritidis, D., Turnock, S., Naik, V., Szopa, S., Georgoulias, A. K., et al. (2022). Climate change penalty and benefit on surface ozone: A global perspective based on CMIP6 earth system models. *Environmental Research Letters*, *17*(2), 024014. https://doi.org/10.1088/1748-9326/ac4a34

References From the Supporting Information

Li, M., Kurokawa, J., Zhang, Q., Woo, J.-H., Morikawa, T., Chatani, S., et al. (2024). MIXv2: A long-term mosaic emission inventory for Asia (2010–2017). *Atmospheric Chemistry and Physics*, *24*(7), 3925–3952. https://doi.org/10.5194/acp-24-3925-2024

Schnell, J. L., Prather, M. J., Josse, B., Naik, V., Horowitz, L. W., Zeng, G., et al. (2016). Effect of climate change on surface ozone over North America, Europe, and East Asia. *Geophysical Research Letters*, *43*(7), 3509–3518. https://doi.org/10.1002/2016GL068060

Zhu, Y., Liu, Y., Li, S., Wang, H., Lu, X., Wang, H., et al. (2024). Assessment of tropospheric ozone simulations in a regional chemical transport model using GEOS-Chem outputs as chemical boundary conditions. *Science of the Total Environment*, *906*, 167485. https://doi.org/10.1016/j.scitotenv.2023.167485

Erratum

The originally published version of this article contained typographical errors. The second affiliation of coauthors Yue Tan and Tao Wang has been corrected as follows: The Hong Kong Polytechnic University Shenzhen Research Institute, Shenzhen, China. Accordingly, the supporting information has been replaced to reflect this correction. In addition, in the first sentence of the fourth paragraph of Section 3.2.2 the citation for Figure 2c has been removed. This may be considered the authoritative version of record.